

Supporting Information for

Iron-loaded Pure Silica -SVR Zeolite for the Hydroxylation of Phenol

Authors:

Wenwen Song^a, Haodong Xie^a, Li Liu^a, Xiang Ni^a, Yuan Xue^a, Yan Liu^a, Junwen Chen^b,
Lei Wang^{a*}, and Hongjun Zhu^{a*}

Affiliations:

^aSchool of Chemistry and Molecular Engineering, Nanjing Tech University, South
Puzhu Rd. 30, Nanjing, 211816, P. R. China.

^bResearch Institute of Petroleum Processing, SINOPEC, Beijing 100083, People's
Republic of China.

***Corresponding Authors:**

I_wang19@njtech.edu.cn (L. Wang)

zhuhj@njtech.edu.cn (H. Zhu)

Table of Contents

1 Figures	3
Fig. S1 Liquid ^1H NMR spectra of hexamethylene-1,6-bis-(N-methyl-N-pyrrolidinyl) bromide in D_2O	3
Fig. S2 Liquid ^{13}C NMR spectra of hexamethylene-1,6-bis-(N-methyl-N-pyrrolidinyl) bromide in D_2O	4
Fig. S3 Calibrated internal standard curves	5
Fig. S4 Pawley fitting profiles	6
Fig. S5 Vacuum FT-IR spectra pattern	7
Fig. S6 Typical high-resolution TEM images	8
Fig. S7 The online gas chromatogram analysis	9
Fig. S8 TG-DTA-DSC profiles.....	10
Fig. S9 Reaction kinetic curves of phenol hydroxylation.....	11
Fig. S10 EPR spectra	12
2 List of tables	13
Table S1 Standard linear equations and correction factors	13
Table S2 The textural pore properties	14
Table S3 The elemental content of Fe/SVR- x catalysts.....	15
Table S4 Direct hydroxylation of different arene substrates with Fe/SVR- x	16
Table S5 Direct hydroxylation of phenol with the different amount of acetic acid.	17
Table S6 Direct hydroxylation of phenol with different type of solvents.	18
Table S7 Comparison of direct hydroxylation of phenol with H_2O_2 with different catalysts. ...	19

1 Figures

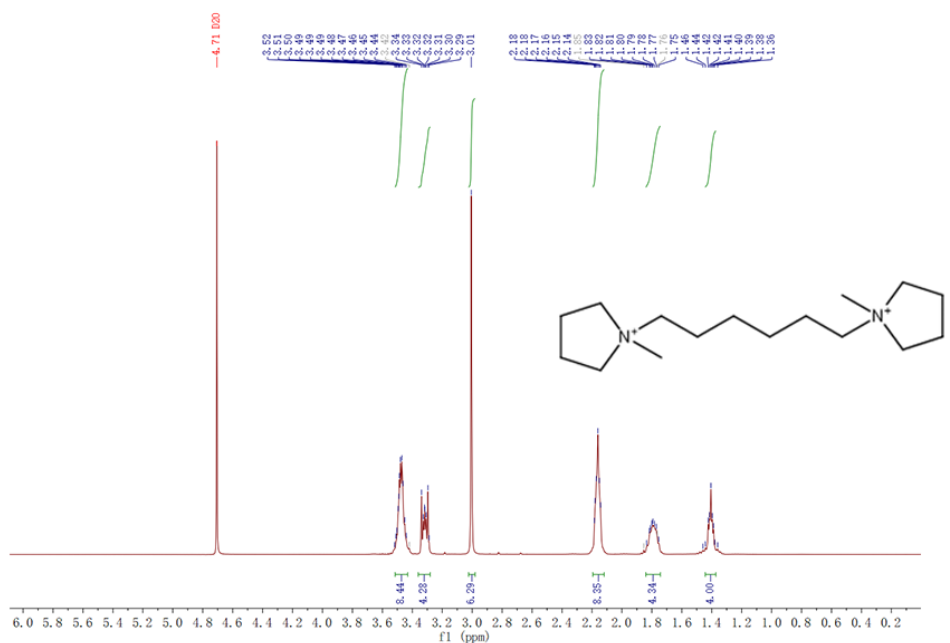


Fig. S1 Liquid ¹H NMR spectra of hexamethylene-1,6-bis-(N-methyl-N-pyrrolidinyl) bromide in ²D₂O.

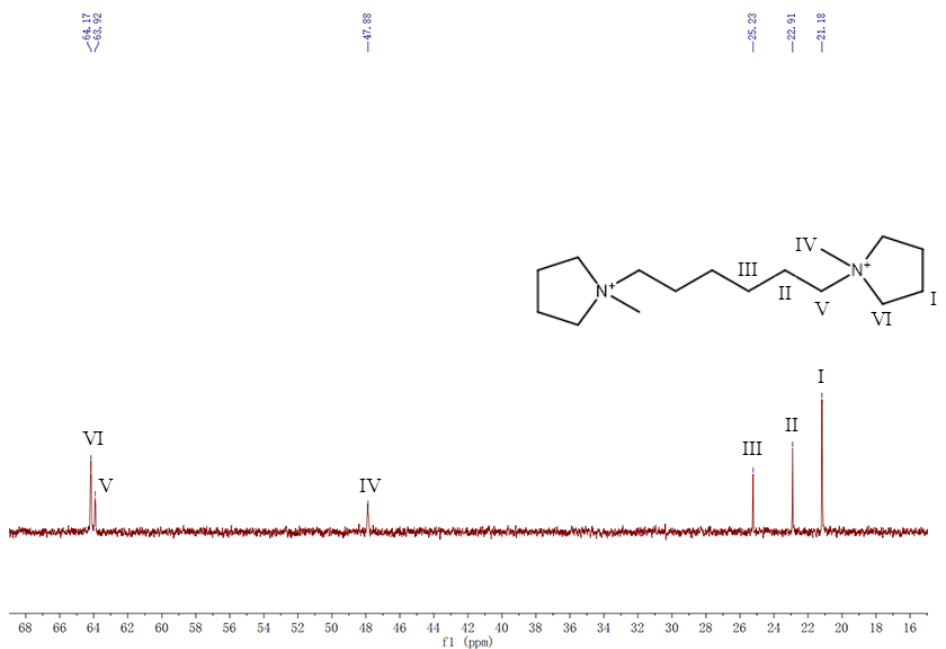


Fig. S2 Liquid ^{13}C NMR spectra of hexamethylene-1,6-bis-(N-methyl-N-pyrrolidinyl) bromide in D_2O .

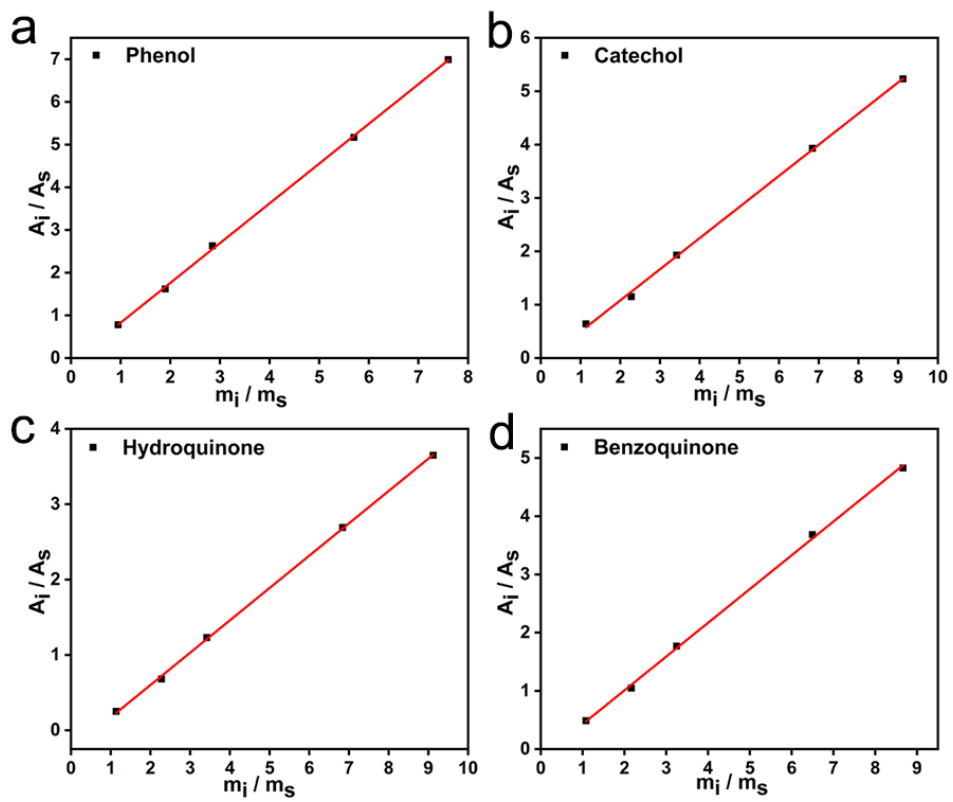


Fig. S3 Calibrated internal standard curves of (a) phenol (b) catechol (c) hydroquinone (d) benzoquinone by GC.

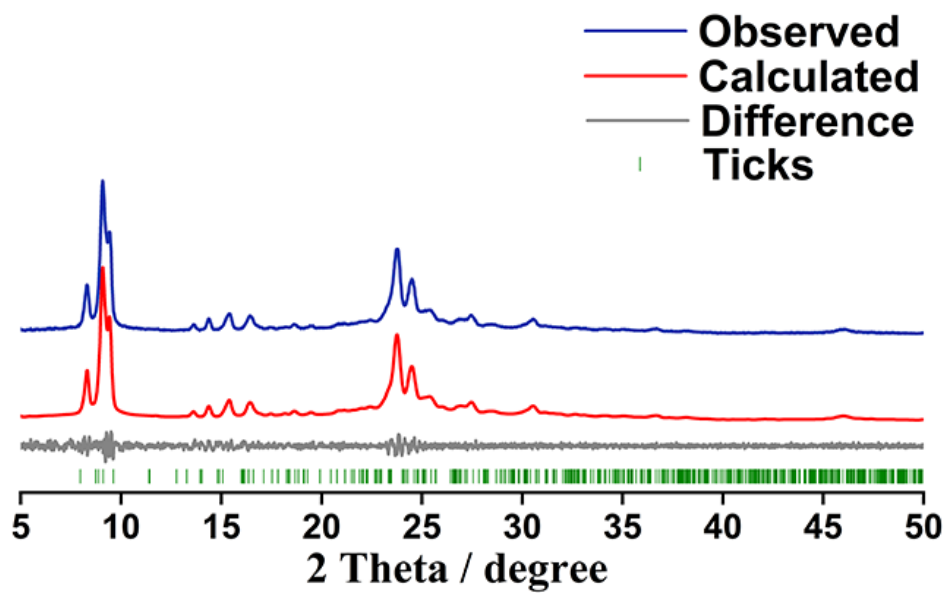


Fig. S4 Pawley fitting profiles of calcined -SVR zeolite (Radiation source: Cu K α_{12} , wavelength: 1.5418 Å), R_{exp} : 2.26%, R_{wp} : 2.22%, GOF: 0.98.

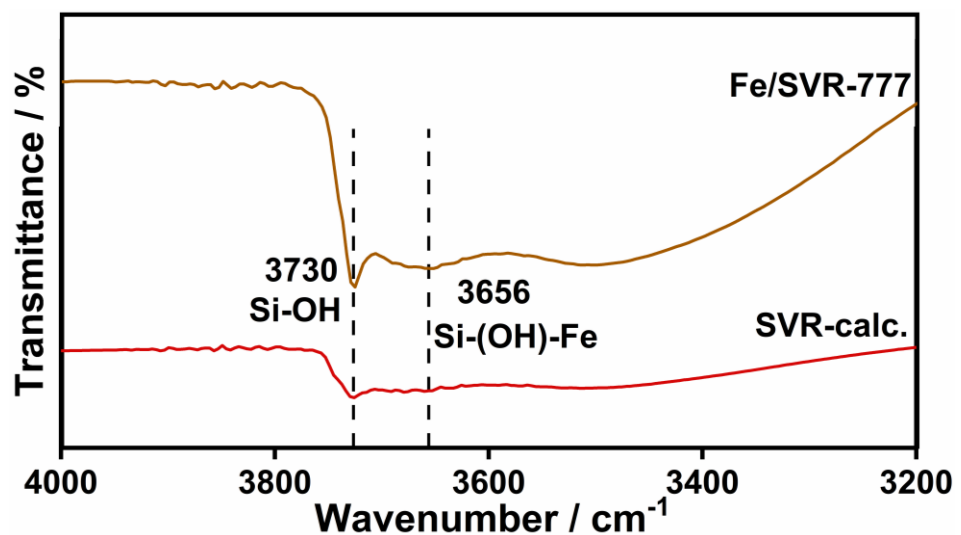


Fig. S5 Vacuum FT-IR spectra pattern of zeolite SVR-calc. and Fe/SVR-777 collected at 303 K.

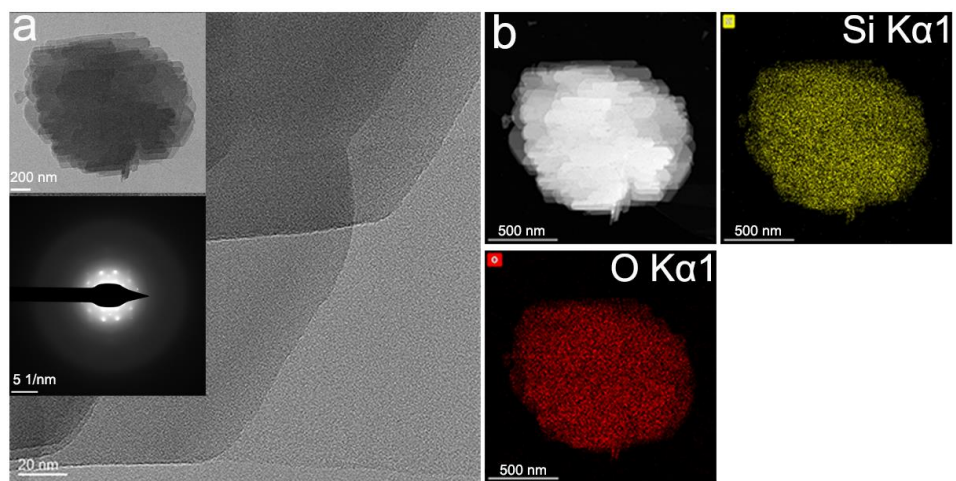


Fig. S6 Typical high-resolution TEM images and element mapping of the calcined -SVR zeolite. (a) High-magnification TEM images of the encircled area, inset: low magnification TEM morphology (top), and electron diffraction pattern (down), (b) element mapping composition elements, respectively.

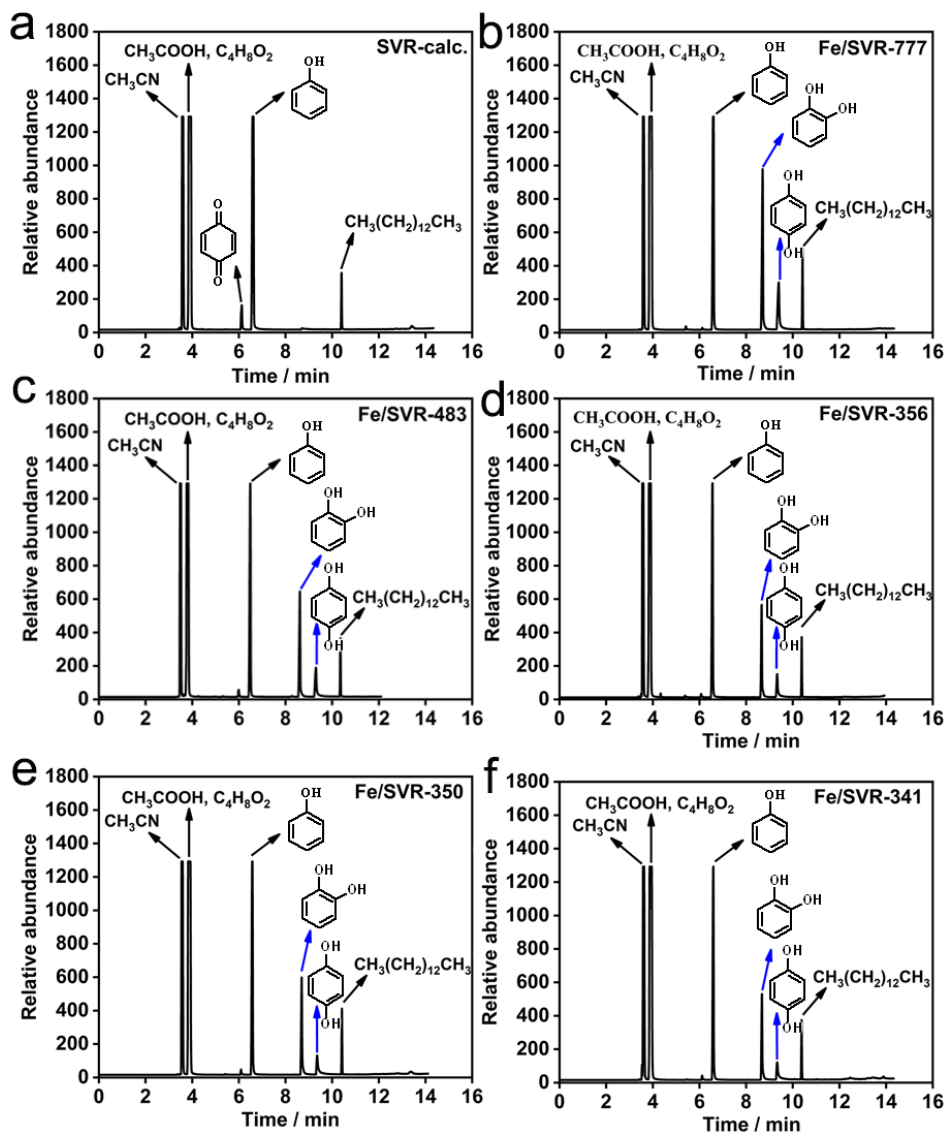


Fig. S7 The online gas chromatogram analysis of phenol hydroxylation products as converted by the Fe/SVR-*x*.

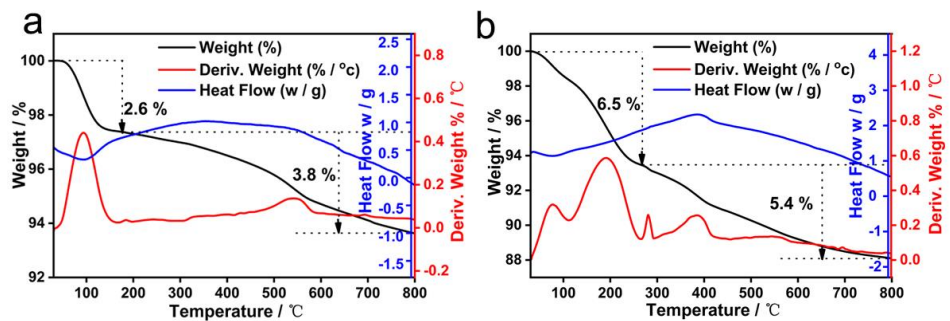


Fig. S8 TG-DTA-DSC profiles of fresh (a) Fe/SVR-777 and the spent (b) Fe/SVR-777.

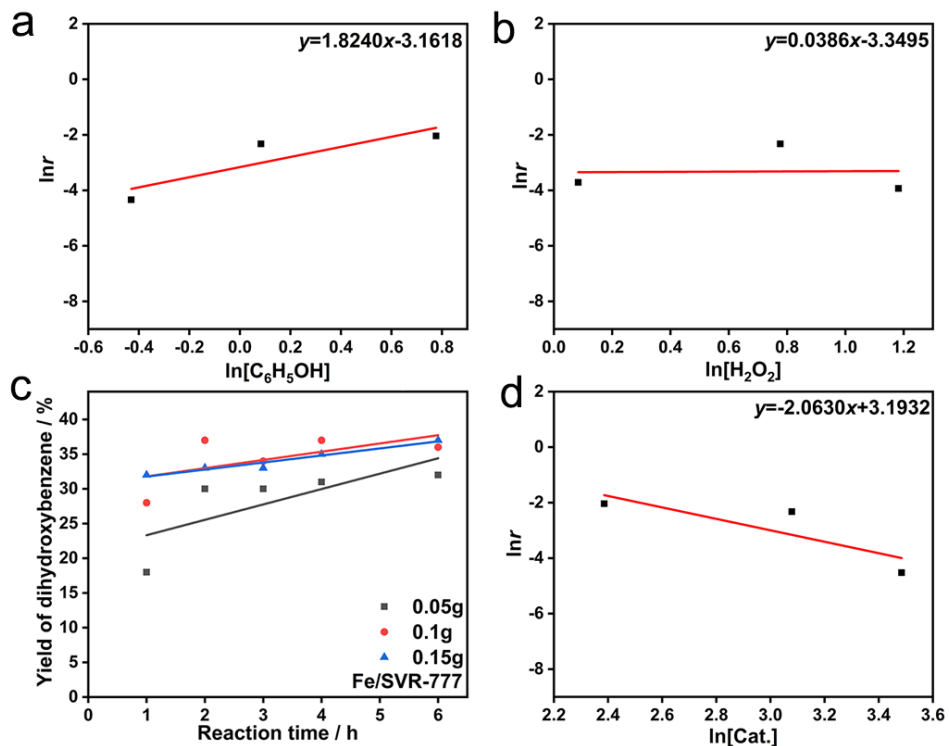


Fig. S9 Reaction kinetic curves of phenol hydroxylation. a) Relationship between initial rate of phenol hydroxylation and phenol concentration (mol/L), b) relationship between initial rate of phenol hydroxylation and H₂O₂ concentration (mol/L), c) yield of dihydroxybenzene with different amount of Fe/SVR-777, d) relationship between initial rate of phenol hydroxylation and catalyst concentration (g/L). Reaction condition: Phenol: 5 mmol, CH₃CN: H₂O: 2 mL: 1.21 mL, CH₃COOH: 0.4 mL, H₂O₂: 1 mL, Fe/SVR-777: 0.1 g, temperature: 353 K. The obtained products were analyzed by GC.

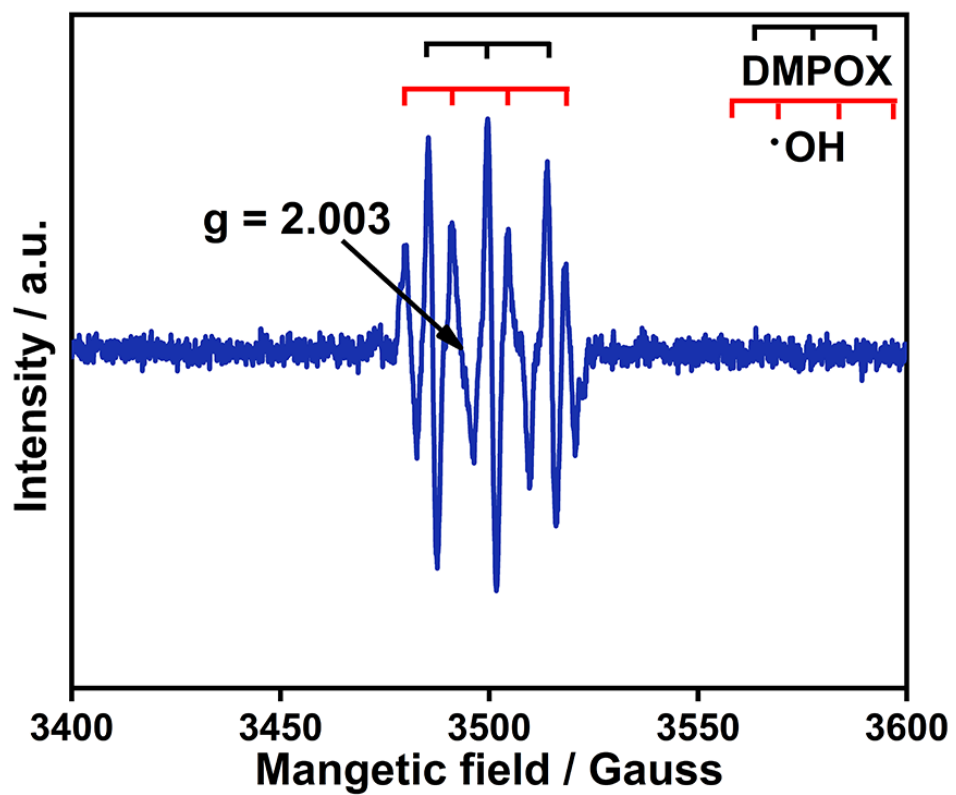


Fig. S10 EPR spectra of DMPO trapped the reacted solution of the Fe/SVR-777 at 40 minutes.

2 List of tables

Table S1 Standard linear equations and correction factors of phenol, catechol, hydroquinone, and benzoquinone.

Entry	Linear equation	R ²	f _{is}
Phenol	$y = 0.92229x - 0.04671$	0.9996	1.0842
Catechol	$y = 0.58695x - 0.10847$	0.9991	1.7037
Hydroquinone	$y = 0.42931x - 0.25765$	0.9997	2.3293
Benzoquinone	$y = 0.58000x - 0.15006$	0.9992	1.7421

Table S2 The textural pore properties of -SVR zeolites evaluated by N₂ sorption at 77 K.

Catalyst	BET surface area (m ² /g) ^a	Langmuir surface area (m ² /g)	Total volume (cm ³ /g) ^b	Micropore volume (cm ³ /g) ^b
SVR-calc.	457	621	0.23	0.15
Fe/SVR-777	415	567	0.21	0.13
Fe/SVR-483	396	543	0.20	0.12
Fe/SVR-356	394	542	0.20	0.12
Fe/SVR-350	396	551	0.20	0.12
Fe/SVR-341	396	553	0.20	0.12

Note: ^aCalculated by the BET method, ^bCalculated by the *t*-plot method.

Table S3 The elemental content of Fe/SVR-*x* catalysts.

Entry	Si/wt%	Fe/wt%
SVR-calc.	45.90	0
Fe/SVR-777	46.61	0.12
Fe/SVR-483	45.92	0.19
Fe/SVR-356	46.28	0.26
Fe/SVR-350	45.51	0.26
Fe/SVR-341	46.08	0.27
Fe/SVR-777 ^a	46.40	0.07

Note: The elemental content of samples was determined using ICP-OES. ^a The elemental content data of the sample was obtained after the phenol hydroxylation reaction.

Table S4 Direct hydroxylation of different arene substrates with Fe/SVR-*x*.

Entry	Substrate	Catalyst	X (%) ^a	Y (%) ^b	S (%) ^c
1	anisole	SVR-calc.	/	/	/
2	anisole	Fe/SVR-777	18	16	88.9
3	anisole	Fe/SVR-350	4	4	99
4	phenol	/	/	/	/
5	phenol	SVR-calc.	5	/	/
6	phenol	Fe/SVR-777	37	37	99
7	phenol	Fe/SVR-483	32	32	96.9
8	phenol	Fe/SVR-356	23.6	23	97.5
9	phenol	Fe/SVR-350	22.8	22	96.5
10	phenol	Fe/SVR-341	21.7	21	96.8

Note: Reaction condition: substrates: 5 mmol, CH₃CN: H₂O: 2 mL: 1.21 mL, CH₃COOH: 0.4 mL, H₂O₂: 1 mL, catalyst: 0.1 g, time: 2 h, temperature: 353 K, the obtained products were analyzed by GC. ^aThe conversion of anisole or phenol, ^bthe yield of 4-methoxyphenol、2-methoxyphenol or dihydroxybenzene, ^cthe selectivity of 4-methoxyphenol 、 2-methoxyphenol or dihydroxybenzene.

Table S5 Direct hydroxylation of phenol with the different amount of acetic acid.

Entry	Additive (mL)	X _{Ph} (%) ^a	Y _{Cat} (%) ^b	Y _{Hy} (%) ^c	S (%) ^d
1	/	12	5	/	41.7
2	0.2	22.6	15	4	84
3	0.3	20.6	14	6	97
4	0.4	37	23	14	99
5	0.5	31	21	9	96.8
6	0.6	27	17	9	96.3
7	0.7	19.7	13	6	96.4

Note: Reaction condition: phenol: 5 mmol, CH₃CN: H₂O: 2 mL: 1.21 mL, additive: CH₃COOH, H₂O₂: 1 mL, Fe/SVR-777: 0.1 g, time: 2 h, temperature: 353 K, the obtained products were analyzed by GC. ^aThe conversion of phenol, ^bthe yield of catechol, ^cthe yield of hydroquinone, ^dthe selectivity of catechol and hydroquinone.

Table S6 Direct hydroxylation of phenol with different type of solvents.

Entry	Solvent	X _{Ph} (%) ^a	Y _{Cat} (%) ^b	Y _{Hy} (%) ^c	S (%) ^d
1	CH ₃ CH ₂ OH	/	/	/	/
2	DMF	/	/	/	/
3	DMSO	/	/	/	/
4	CH ₃ COOCH ₂ CH ₃	16	13	3	93
5	CH ₃ CN	20	14	6	93
6	H ₂ O	27	19	8	97.5
7	CH ₃ COOCH ₂ CH ₃ / H ₂ O	4	4	/	47.6
8	CH ₃ CN / H ₂ O	37	23	14	99

Note: Reaction condition: phenol: 5 mmol, solvent: 3.21 mL, CH₃COOH: 0.4 mL, H₂O₂: 1 mL, Fe/SVR-777: 0.1 g, time: 2 h, temperature: 353 K, the obtained products were analyzed by GC.

^aThe conversion of phenol, ^bthe yield of catechol, ^cthe yield of hydroquinone, ^dthe selectivity of catechol and hydroquinone.

Table S7 Comparison of direct hydroxylation of phenol with H₂O₂ with different catalysts.

Entry	Catalyst	Type	Time / h	X (%) ^a	Y (%) ^b	S (%) ^c	Ref.
1	Fe/HY	Zeolite	1	48	33.6	70	1
2	MSCu	Porous material	5	52	29	58	2
3	Fe-MCM-41	Zeolite	4	53	31.8	60	3
4	Cu-SBA-15	Zeolite	3.5	50	27.5	55	4
5	Fe/AC	Catalyst	1	41.3	36	87	5
6	HPB-TS-1	Zeolite	4	21.3	20	94.5	6
7	TS-1	Zeolite	0.5	27.3	27	99	7
8	TS-1	Zeolite	6	31.6	31.6	99	8
9	Cu-SCPN	Polymeric Nanoparticles	1	30	15.6	51.4	9
10	Au / ZnO	photocatalysis	3	50	20	40	10
11	Fe/FSM-16	Zeolite	6	29	27	94.5	11
12	Fe-ZSM-5	Zeolite	4	40	34	86	12
13	Fe/SAC	Monatomic catalyst	0.5	53	47	88	13
14	Fe-NW-ZSM-5	Zeolite	12	26	26	99	14
15	NiV-LDH-NS	electrocatalysis	9	72	56	78	15
16	CMS-F(P)	Zeolite	2	29.6	25	85.1	16
17	ZrAPO-41/2	Zeolite	20	18.2	14.4	79.1	17
18	Fe/SVR- <i>x</i>	Zeolite	2	37	37	99	This work

Note: ^aThe conversion of phenol, ^bthe yield of dihydroxybenzene, ^cthe selectivity of dihydroxybenzene.

References:

1. J. Long, X. Wang, Z. Ding, Z. Zhang, H. Lin, W. Dai and X. Fu, *J. Catal.*, 2009, **264**, 163-174.
2. J. Tang, H. Xin, W. Su, J. Liu, C. Li and Q. Yang, *Chinese J.Catal.*, 2010, **31**, 386-393.
3. S. V. Sirotin, I. F. Moskovskaya and B. V. Romanovsky, *Catal. Sci. Technol.*, 2011, **1**, 971-980.
4. H. Zhang, C. Tang, Y. Lv, C. Sun, F. Gao, L. Dong and Y. Chen, *J. Colloid Interf. Sci.*, 2012, **380**, 16-24.
5. M. Jin, R. Yang, M. Zhao, G. Li and C. Hu, *Ind. Eng. Chem. Res.*, 2014, **53**, 2932-2939.
6. W. Cheng, Y. Jiang, X. Xu, Y. Wang, K. Lin and P. P. Pescarmona, *J. Catal.*, 2016, **333**, 139-148.
7. B. Wang, M. Lin, X. Peng, B. Zhu and X. Shu, *RSC Adv.*, 2016, **6**, 44963-44971.
8. Y. Zuo, M. Liu, M. Ma, Y. Wang, X. Guo and C. Song, *ChemistrySelect*, 2016, **1**, 6160-6166.
9. S. Thanneeru, S. S. Duay, L. Jin, Y. Fu, A. M. Angeles-Boza and J. He, *ACS Macro Lett.*, 2017, **6**, 652-656.
10. F. Lin, B. E. Cojocaru, L. S. Williams, C. A. Cadigan, C. Tian, M. N. Grecu, H. L. Xin, S. Vyas, V. I. Parvulescu and R. M. Richards, *Nanoscale*, 2017, **9**, 9359-9364.
11. G. Luo, Y. Jiao, X. Lv, X. Zhang and X. Gao, *Chem. Intermediat.*, 2018, **44**, 5377-5387.
12. Z. Han, F. Zhang and X. Zhao, *Microporous Mesoporous Mat.*, 2019, **290**, 109679.
13. M.-X. Gu, X.-Q. Zheng, S.-S. Peng, S.-C. Qi, X.-Q. Liu and L.-B. Sun, *ACS Sustain. Chem. Eng.*, 2023, **11**, 7844-7850.
14. Y. Shen, H. Li, X. Zhang, X. Wang and G. Lv, *Nanoscale*, 2020, **12**, 5824-5828.
15. G. Li, Y. Xu, H. Pan, X. Xie, R. Chen, D. Wu and L. Wang, *J. Mater. Chem. A*, 2022, **10**, 6748-6761.
16. S. Li, G. Li, G. Li, G. Wu and C. Hu, *Microporous Mesoporous Mat.*, 2011, **143**, 22-29.
17. D. Chakrabortty, J. N. Ganguli and C. V. V. Satyanarayana, *Microporous Mesoporous Mat.*, 2011, **137**, 65-71.